Eksakta : Berkala Ilmiah Bidang MIPA
VOLUME 26 NO 04 2025, pp 480-499
ISSN : Print 1411-3724 — Online 2549-7464
DOI : https://doi.org/10.24036/eksakta/vol26-iss04/631

Eksakta
Berkala Ilmiah Bidang MIPA
http://www.eksakta.ppj.unp.ac.id/index.php/eksakta

Article

In Silico Evaluation of Natural Compounds as Dual Inhibitors of Exotoxin A and LasB (Elastase) Virulence Proteins in *Pseudomonas aeruginosa*

Andrias Bayu Fariska[1,2], Linda Erlina[3*], Ade Arsianti[3], Aryo Tedjo[3]

[1]Master Programs in Biomedical Sciences, Faculty of Medicine, Universitas Indonesia, Jakarta, Indonesia
[2]Balai Besar Biomedis dan Genomika Kesehatan (BBBinomika), Jakarta, Indonesia
[3]Department of Medical Chemistry, Faculty of Medicine, Universitas Indonesia, Jakarta, Indonesia

Article Info

Article history :
Received October 26, 2025
Revised Novenber 10, 2025
Accepted November 13, 2025
Published December 30, 2025

Keywords :
Pseudomonas aeruginosa,
exotoxin A,
lasB,
molecular docking,
herbalDB,

Abstract. *Pseudomonas aeruginosa* is an opportunistic pathogen whose virulence is largely mediated by Exotoxin A and LasB (elastase), making them promising anti-virulence drug targets. This study aimed to evaluate the inhibitory potential of natural compounds against these two key proteins using an in silico approach. Pharmacophore-based virtual screening of HerbalDB compounds was performed by LigandScout software, followed by molecular docking using AutoDockTools-1.5.7 against Exotoxin A (PDB ID: 1AER) and LasB (PDB ID: 1U4G). Native ligands and co-crystallized inhibitors were used as docking controls to validate binding accuracy. Among the screened compounds, Epicatechin-(4β-6)-epicatechin-(4β-8)-catechin exhibited the strongest binding affinity to Exotoxin A ($\Delta G = -10.72$ kcal·mol^{-1}), while Carpaine showed the highest affinity for LasB ($\Delta G = -8.91$ kcal·mol^{-1}). The predicted interactions involved hydrogen bonds and hydrophobic interactions with active-site residues, comparable to the native inhibitors. Furthermore, ADMET analysis indicated favorable pharmacokinetic and drug-likeness properties. These findings suggest that selected natural compounds possess potential dual inhibitory activity against Exotoxin A and LasB, warranting further experimental validation as anti-virulence candidates for controlling *P. aeruginosa* infections.

Corresponding Author :
Linda Erlina
Department of Medical Chemistry, Faculty of Medicine, Universitas Indonesia, Jakarta, Indonesia
Email : linda.erlina22@ui.ac.id

1. Introduction

Pseudomonas aeruginosa is an opportunistic Gram-negative pathogen that possess a major threat to immunocompromised patients and individuals with chronic infections such as cystic fibrosis, burn wounds, and ventilator-associated pneumonia [1-2]. Its remarkable ability to form biofilms and secrete multiple virulence factors contributes to persistent infections and resistance to conventional antibiotics. Among its virulence determinants, Exotoxin A (ETA) and LasB (elastase) are considered key pathogenic proteins responsible for host tissue destruction, immune evasion, and bacterial survival during infection. Exotoxin A acts by catalyzing the ADP-ribosylation of elongation factor 2 (EF-2), leading to inhibition of host protein synthesis and cell death [3]. Whereas LasB, a zinc-dependent metalloprotease, degrades structural proteins such as elastin, collagen, and immunoglobulins, resulting in severe tissue damage [4].

The increasing prevalence of multidrug-resistant *P. aeruginosa* strains has limited the efficacy of current antibiotics, highlighting the urgent need for alternative therapeutic strategies that attenuate bacterial virulence rather than viability [5]. Anti-virulence therapy, which aims to disarm the pathogen without exerting strong selective pressure for resistance, has emerged as a promising approach. Naturally derived bioactive molecules, owing to their structural diversity and broad pharmacological potential, are a valuable resource for developing novel anti-virulence agents [6].

Computational (in silico) techniques such as pharmacophore modeling, virtual screening, and molecular docking offer efficient approaches for identifying potential inhibitors targeting bacterial virulence proteins [7-8]. These approaches can predict molecular interactions and binding affinities between bioactive compounds and their targets, accelerating the discovery of promising inhibitors. However, no previous study has simultaneously investigated both Exotoxin A and LasB as dual virulence targets using compounds from the HerbalDB database. This gap underscores the novelty and importance of exploring HerbalDB-derived phytochemicals, which represent unique Indonesian medicinal plant compounds with diverse chemical scaffolds and untapped therapeutic potential.

The objective of this study is to evaluate the inhibitory potential of selected HerbalDB natural compounds against both Exotoxin A and LasB proteins of *P. aeruginosa* using an in silico structure-based approach. Pharmacophore-based virtual screening was performed using LigandScout, followed by molecular docking and ADMET analysis to identify dual-target natural inhibitors with potential anti-virulence activity.

2. Experimental Section

2.1. Materials

This study employed a structure-based in silico approach using publicly available protein and ligand data. The three-dimensional crystal structures of *Pseudomonas aeruginosa* Exotoxin A and LasB (elastase) were retrieved from the Protein Data Bank (PDB) under accession codes 1AER and 1U4G, respectively. The native co-crystallized inhibitors from each PDB structure were used as reference ligands to validate the docking protocol and compare binding affinities.

Natural compounds used as test ligands were obtained from the HerbalDB database, an Indonesian medicinal plant repository that containing three-dimensional molecular structures of phytochemicals in SDF format [9]. Compounds were selected based on pharmacophore features relevant to enzyme inhibition, virtual screening of compounds from the HerbalDB database was conducted using LigandScout 4.5 software, and then optimized prior to docking. The structures were energy-minimized using Open Babel (integrated in PyRx 0.8) to convert and prepare ligand files in PDBQT format.

All docking simulations were carried out using AutoDockTools-1.5.7. The protein structures were preprocessed by removing water molecules, adding polar hydrogens, and assigning Gasteiger charges. Ligand and receptor grid parameters were defined to cover the active site region identified from the native ligand position. Visualization and analysis of docking conformations, hydrogen bonding, and hydrophobic interactions were performed using Ligplot+ v.2.2.9 software.

This study followed a structure-based drug discovery (SBDD) workflow integrating pharmacophore screening, molecular docking, and ADMET analysis to identify potential natural inhibitors of *Pseudomonas aeruginosa* virulence proteins Exotoxin A and LasB (elastase). The overall research workflow is illustrated in the schematic flowchart of Figure 1.

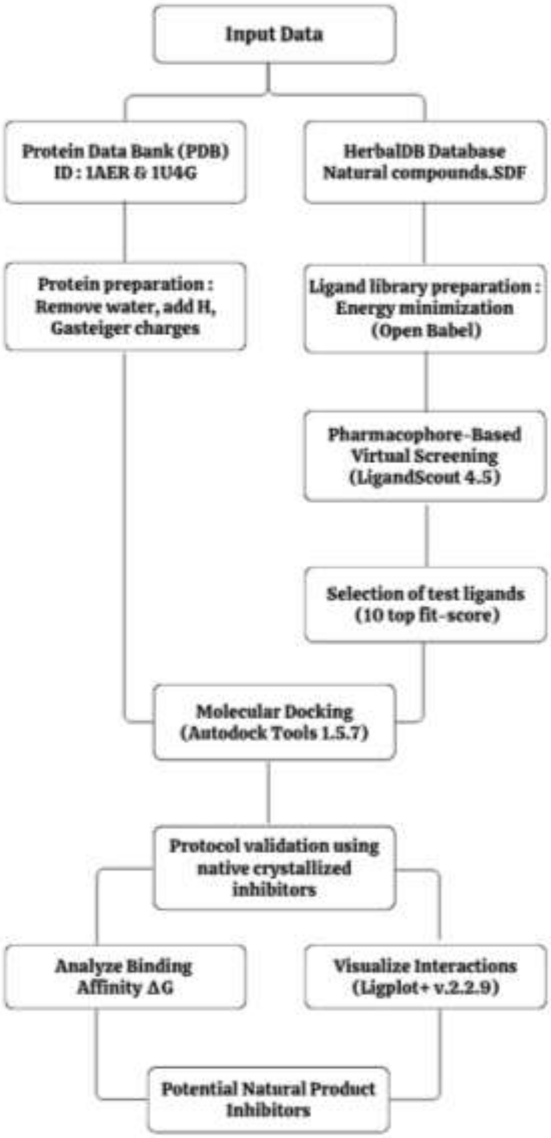

Figure 1. Schematic/Flowchart of research

2.2. Methods

2.2.1. Structure-Based Drug Discovery

Initially, a comprehensive literature study was conducted to identify *P. aeruginosa* virulence factors and previously reported inhibitors. Subsequently, the three-dimensional (3D) crystal structures of Exotoxin A with TAD native ligand (PDB ID: 1AER, Table 1 and Figure 2) and LasB with HPI native ligand (PDB ID: 1U4G Table 1 and Figure 3) were retrieved from the Protein Data Bank (PDB, https://www.rcsb.org/) [10-11]. The native co-crystallized ligands within each structure were used as docking controls to validate docking accuracy and assess protocol reliability.

Table 1. Characteristics of protein target Exotoxin A proteins with TAD Native Ligand (PDB: 1AER) and protein target Elastase with HPI Native Ligand (PDB: 1U4G)

Structure summary	PDB ID	
	ADP-Ribosylation_1AER	Hydrolase_1U4G
Method	X-Ray diffraction	X-Ray diffraction
Organism	*Pseudomonas aeruginosa*	*Pseudomonas aeruginosa*
Resolution	2.30 Å	1.40 Å
Molecule	Exotoxin A	Elastase
Chains	A, B	A
Sequence Length	211	301
Mutations	0	0
Native ligands	TAD (Beta-Methylene-Thiazole-4-Carboxyamide-Adenine Dinucleotide)	HPI (N-(1-Carboxy-3-Phenylpropyl)Phenylalanyl-Alpha-Asparagine

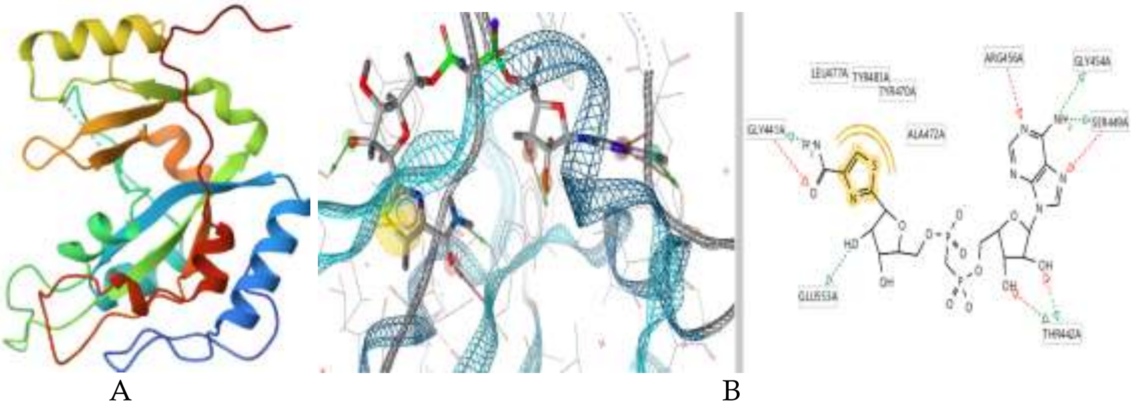

Figure 2. A) 3D Structure of Exotoxin A proteins with TAD native ligand, PDB ID: 1AER and B) Fitur pharmacophore native ligand TAD

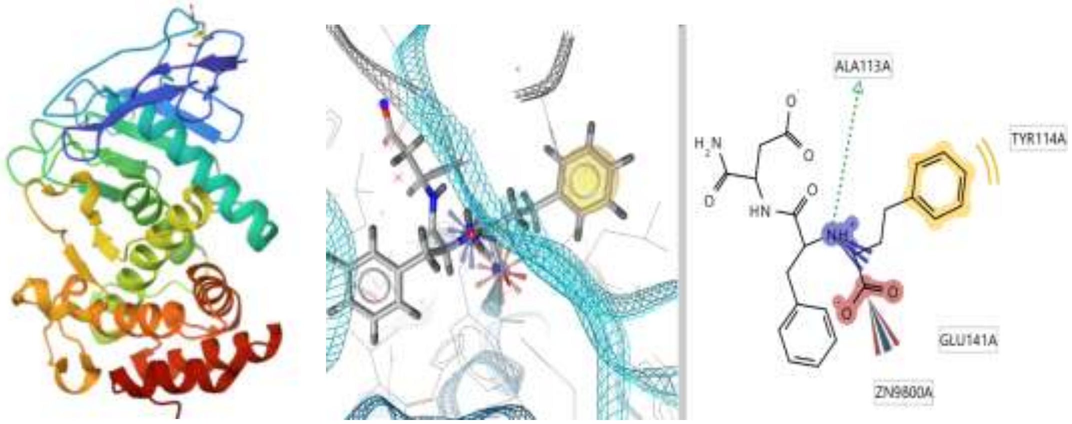

A B

Figure 3. A) 3D Structure of Elastase proteins with HPI native ligand, PDB ID: 1U4G and B) Fitur pharmacophore native ligand HPI

2.2.2. Ligand and Macromolecule Preparation

A total of 1,500 natural compounds from the HerbalDB database an Indonesian medicinal plant repository containing three-dimensional molecular structures of phytochemicals in SDF format were initially screened based on pharmacophore features relevant to enzyme inhibition. Pharmacophore-based virtual screening was performed using LigandScout 4.5 software with the pharmacophore-fit scoring function set to "match all query features," and the top ten compounds with the highest scores were selected for further molecular docking analysis. Each selected ligand was energy-minimized using Open Babel (integrated in PyRx 0.8) and converted to PDBQT format with proper protonation and stereochemical configuration.

The crystal structures of *Pseudomonas aeruginosa* Exotoxin A (PDB ID: 1AER) and LasB (elastase, PDB ID: 1U4G) were retrieved from the Protein Data Bank (PDB). Prior to docking, both protein structures were prepared by removing water molecules, adding polar hydrogens, and assigning Gasteiger charges using AutoDockTools-1.5.7. The active site regions were defined by a grid box covering the native ligand binding pocket with sufficient margin to allow ligand flexibility. Molecular docking was performed with AutoDock 4.2 using the Lamarckian Genetic Algorithm (LGA), with 100 runs per ligand, a population size of 150, and 2.5×10^6 energy evaluations. Docking accuracy was validated through re-docking of native ligands, and the resulting conformations were analyzed for hydrogen bonding and hydrophobic interactions using Ligplot+ v.2.2.9.

2.2.3. Molecular Docking

Docking accuracy was validated by re-docking the native ligand into its original binding site, and the root mean square deviation (RMSD) between the experimental and predicted poses was calculated. An RMSD value of less than 2.0 Å was considered indicative of reliable docking performance. The best binding poses were selected based on the lowest binding energy (ΔG, kcal·mol^{-1}) and consistent orientation within the active site. Post-docking analyses included visualization of ligand–protein interactions such as hydrogen bonding, hydrophobic contacts, and π–π stacking using Ligplot$^+$ v.2.2.9 software. The binding residues were compared with those of the co-crystallized inhibitors to confirm interaction similarity.

2.2.4. Toxicological and Pharmacokinetic Analysis

Toxicological and pharmacokinetic properties were assessed based on Lipinski's Rule of Five and ADMET (absorption, distribution, metabolism, excretion, and toxicity) parameters. The predictions were carried out using the pkCSM web server (https://biosig.lab.uq.edu.au/pkcsm/prediction). The top three compounds from molecular docking were evaluated to estimate their biological and environmental interaction profiles.

3. Results and Discussion

This study successfully identified several natural compounds from HerbalDB with strong binding affinities to *Pseudomonas aeruginosa* Exotoxin A (PDB ID: 1AER) and LasB (PDB ID: 1U4G). Structure-Based Pharmacophore Modelling (SBPM) is a drug discovery approach which is designed to identify key chemical features of a ligand based on the three-dimensional structure of the protein–ligand complex. This method enables spatial visualization and analysis of molecular interactions, which can be utilized for virtual screening, drug optimization, and designing of novel bioactive compounds [12-13]. One of the most widely used software tools for this analysis is LigandScout, which allows for the extraction and visualization of pharmacophore features from the 3D structure of a protein–ligand complex and presents them in an intuitive 2D representation [14-15]. In this study, virtual screening was performed by replacing the default screening database with HerbalDB_best.ldb, which contains a curated dataset of natural compounds derived from medicinal plants. The structure-based pharmacophore modeling (SBPM) virtual screening of HerbalDB yielded ten hit compounds, as summarized in Table 2.

Table 2. The Top 10 hit compounds from screening SBPM

ADP-Ribosylation_1AER			
No	Ligand Code	Compound Name	Pharmacophore-Fit Score
1	Ligand_1	Epicatechin-(4beta-6)-epicatechin-(4beta-8)-catechin	56.36
2	Ligand_2	Theasaponin E2.mol	56.12
3	Ligand_3	Woodfordin C.mol	56.11
4	Ligand_4	Maysin.mol	56.11
5	Ligand_5	Gambiriin B3.mol	56.10
6	Ligand_6	Luteolin 3' –methyl ether 7-mannosyl-(1,2)-alloside.mol	56.05
7	Ligand_7	Eriodictin.mol	56.01
8	Ligand_8	Scutellarein 7-glucsyl-(1-4)-rhamnoside.mol	55.92
9	Ligand_9	3-O-Galloylepigallocatechin-(4beta-8)-epigallocatechin	55.89
10	Ligand_10	3'-O-Methylmaysin.mol	55.87
Hydrolase_1U4G			
No	Ligand Code	Compound Name	Pharmacophore-Fit Score
1	Ligand_1	S-[(E)-Prop-1-enyl]-L-cysteine S-oxide.mol	57.48
2	Ligand_2	L-Tryptophan.mol	56.58
3	Ligand_3	Alliin.mol	56.42
4	Ligand_4	L-Theanine.mol	55.48
5	Ligand_5	Carpaine.mol	47.32

6	Ligand_6	Myricetin 3-(2G-rhamnosylrutinoside).mol	47.05
7	Ligand_7	(-)-2-Norlimacine.mol	46.63
8	Ligand_8	5-Hydroxy-6-oxocoronaridine.mol	46.41
9	Ligand_9	DIMBOA glucoside.mol	45.78
10	Ligand_10	8-Hydroxyapigenin 8(2”,4”-disulfatoglucuronide).mol	45.11

Molecular docking was performed to determine the interaction between the target protein and the ligand. However, before conducting docking with the test ligands, a validation step was carried out by re-docking the target protein (1AER & 1U4G) with its native ligand [16,17]. Based on the re-docking results presented in Table 3, the grid box size that best met the validation criteria was 60 × 60 × 60 with ga_run 10 in validation III for target protein 1AER and 40 x 40 x 40 with ga_run 15 in validation I for target protein 1U4G, with a binding energy value of −7.34 kcal·mol^{-1} and an RMSD value of 2.83 Å for target protein 1AER and a binding energy value of −7.63 kcal·mol^{-1} and an RMSD value of 1.39 Å for target protein 1U4G. These results represent the most optimal parameters, characterized by the lowest binding energy and RMSD values. The grid coordinates used for this docking validation were x = 52.992; y = 72.529; z = 13.412 for target protein 1AER and x = 18.02; y = 29.164; z = -3.897 for target protein 1U4G.

Table 3. The results of grid box validation from size 40 × 40 × 40; size 50 × 50 × 50; and size 60 × 60 ×60

ADP-Ribosylation_1AER

No	Validation	Grid Box	Binding Energy (kcal/mol)	Ref RMSD (Å)	Inhibition Const (uM)	ga_run
1	I	40x40x40	-2.37	3.02	1.32	10
2	II	50x50x50	-4.03	3.59	715.56	10
3	III	60x60x60	-7.34	2.83	33.23	10

Hydrolase_1U4G

No	Validation	Grid Box	Binding Energy (kcal/mol)	Ref RMSD (A)	Inhibition Const (uM)	ga_run
1	I	40x40x40	-7.63	1.39	2.55	15
2	II	50x50x50	-5,31	3,14	33.58	10
3	III	60x60x60	-6,37	2,76	1.78	10

After obtaining the most appropriate grid box parameters from the validation process, molecular docking was subsequently performed for the target proteins 1AER and 1U4G against the ten selected test ligands with the best pharmacophore fit scores. Following pharmacophore-based screening of 1,500 compounds, the top ten ligands with the highest pharmacophore-fit scores were subjected to molecular docking. Among these, Epicatechin-(4β-6)-epicatechin-(4β-8)-catechin showed the most favorable binding affinity toward Exotoxin A (ΔG = −10.72 kcal·mol^{-1}), while Carpaine exhibited the strongest interaction with LasB (ΔG = −8.91 kcal·mol^{-1}). The lower binding energy values indicate higher binding affinity and greater potential inhibitory strength against the target enzymes. The results are presented in Table 4 and to better visualize the comparative results, Figure 4 presents a bar chart illustrating the binding energies (ΔG) of the top ten compounds for each target protein. This visualization highlights Epicatechin and Carpaine as the most stable ligand–protein complexes among the screened candidates.

Table 4. Lowest binding energy of 10 hit compounds

ADP-Ribosylation_1AER

No	Ligand Code	Compound	Binding Energy (ΔG) (kcal/mol)
1	Ligand_1	Epicatechin-(4beta-6)-epicatechin-(4beta-8)-catechin	-10.72
2	Ligand_2	Theasaponin E2.mol	-1.51
3	Ligand_3	Woodfordin C.mol	-4.48
4	Ligand_4	Maysin.mol	-7.76
5	Ligand_5	Gambiriin B3.mol	-7.93
6	Ligand_6	Luteolin 3' –methyl ether 7-mannosyl-(1,2)-alloside.mol	-6.40
7	Ligand_7	Eriodictin.mol	-9.04
8	Ligand_8	Scutellarein 7-glucsyl-(1-4)-rhamnoside.mol	-8.27
9	Ligand_9	3-O-Galloylepigallocatechin-(4beta-8)-epigallocatechin	-6.70
10	Ligand_10	3'-O-Methylmaysin.mol	-7.22

Hydrolase_1U4G

No	Ligand Code	Compound	Binding Energy (ΔG) (kcal/mol)
1	Ligand_1	S-[(E)-Prop-1-enyl]-L-cysteine S-oxide.mol	-5.78
2	Ligand_2	L-Tryptophan.mol	-7.06
3	Ligand_3	Alliin.mol	-5.74
4	Ligand_4	L-Theanine.mol	-5.89
5	Ligand_5	Carpaine.mol	-8.91
6	Ligand_6	Myricetin 3-(2G-rhamnosylrutinoside).mol	-7.08
7	Ligand_7	(-)-2-Norlimacine.mol	-6.02
8	Ligand_8	5-Hydroxy-6-oxocoronaridine.mol	-7.67
9	Ligand_9	DIMBOA glucoside.mol	-6.85
10	Ligand_10	8-Hydroxyapigenin 8(2",4" disulfatoglucuronide).mol	-2.92

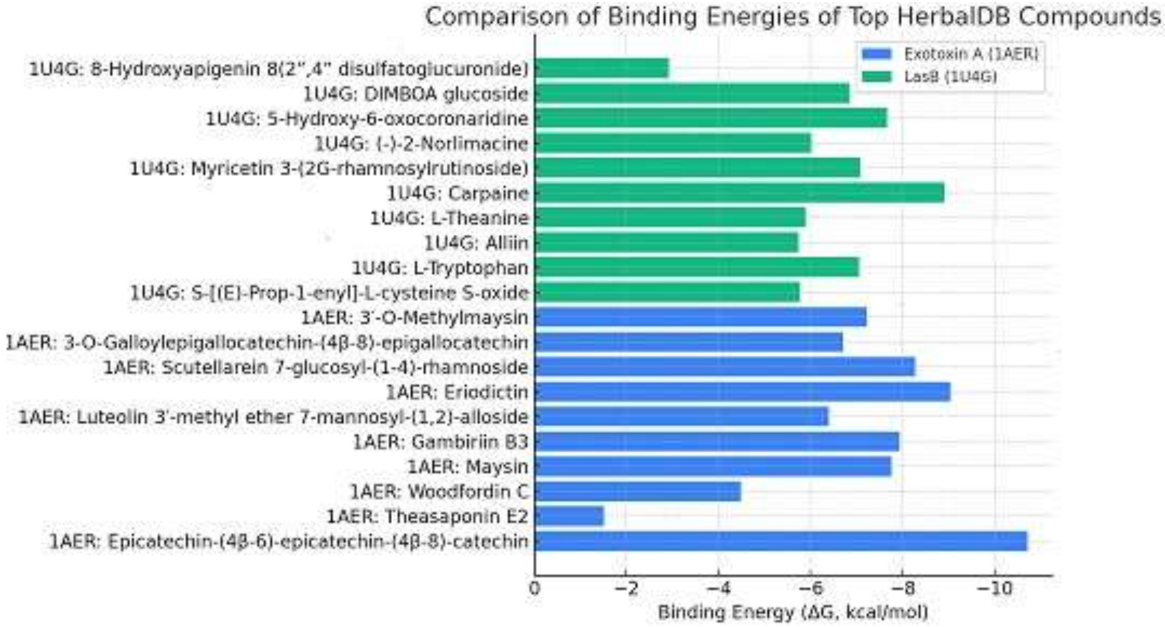

Figure 4. Comparison of binding energies (ΔG) of the top ten compounds against Exotoxin A and LasB targets.

Following the identification of top-ranking compounds based on binding energy, their interactions at the active sites were examined through validated docking and virtual screening results, and subsequently visualized using LigPlot+ v2.2.9. The binding interactions between the native ligand and the target receptor were first analyzed to establish a reference, after which interactions between the selected bioactive compounds (with the lowest binding energies) and the 1AER and 1U4G proteins were evaluated, with emphasis on hydrogen bond distances (See Figure 5 and Figure 6). After that, we compared and analyzed the interactions between the protein/macromolecule and top 3 ligands with lowest binding energy as shown in Table 5.

The analysis revealed that the predominant interactions involved non-covalent forces, particularly hydrogen bonding and hydrophobic interactions, which play a crucial role in stabilizing ligands within the open conformations of protein structures. Hydrogen bonds specifically occur when hydrogen atoms covalently attached to electronegative donor atoms interact with electronegative acceptor atoms. These bonds are especially critical in proteins, commonly forming between the NH and CO groups of α-helical backbones. Such hydrogen bonds are central to the specificity and directionality of molecular interactions between macromolecules (e.g., proteins, nucleic acids) and their ligands, including substrates, inhibitors, and effectors. Consequently, they are essential for accurate molecular recognition in biological systems [18–21].

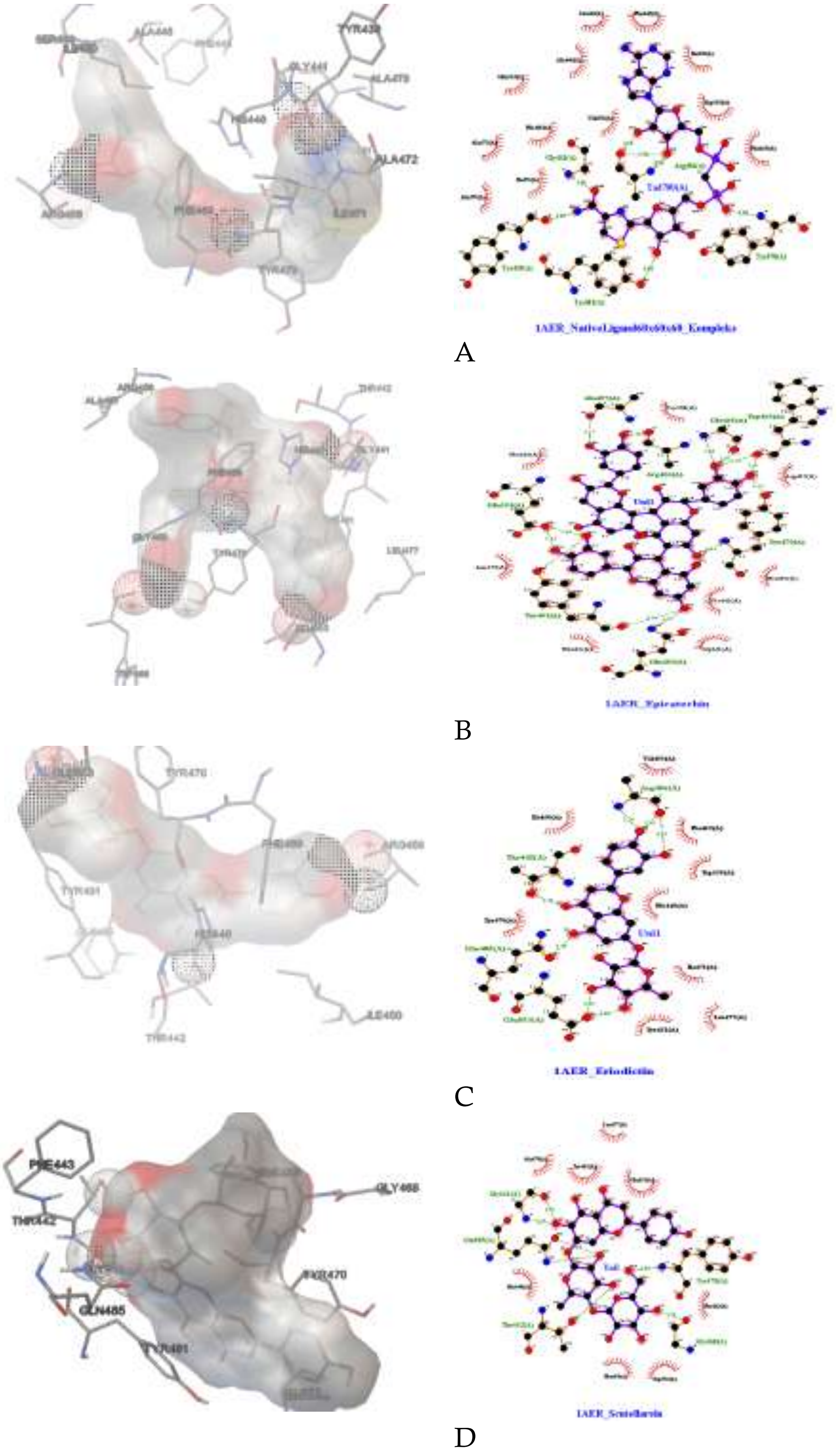

Figure 5. A) Visualization of 3D and 2D molecular docking results for the native ligand compounds TAD, B) Epicatechin-(4beta-6)-epicatechin-(4beta-8)-catechin, C) Eriodictin and D) Scutellarein 7-glucsyl-(1-4)-rhamnoside.

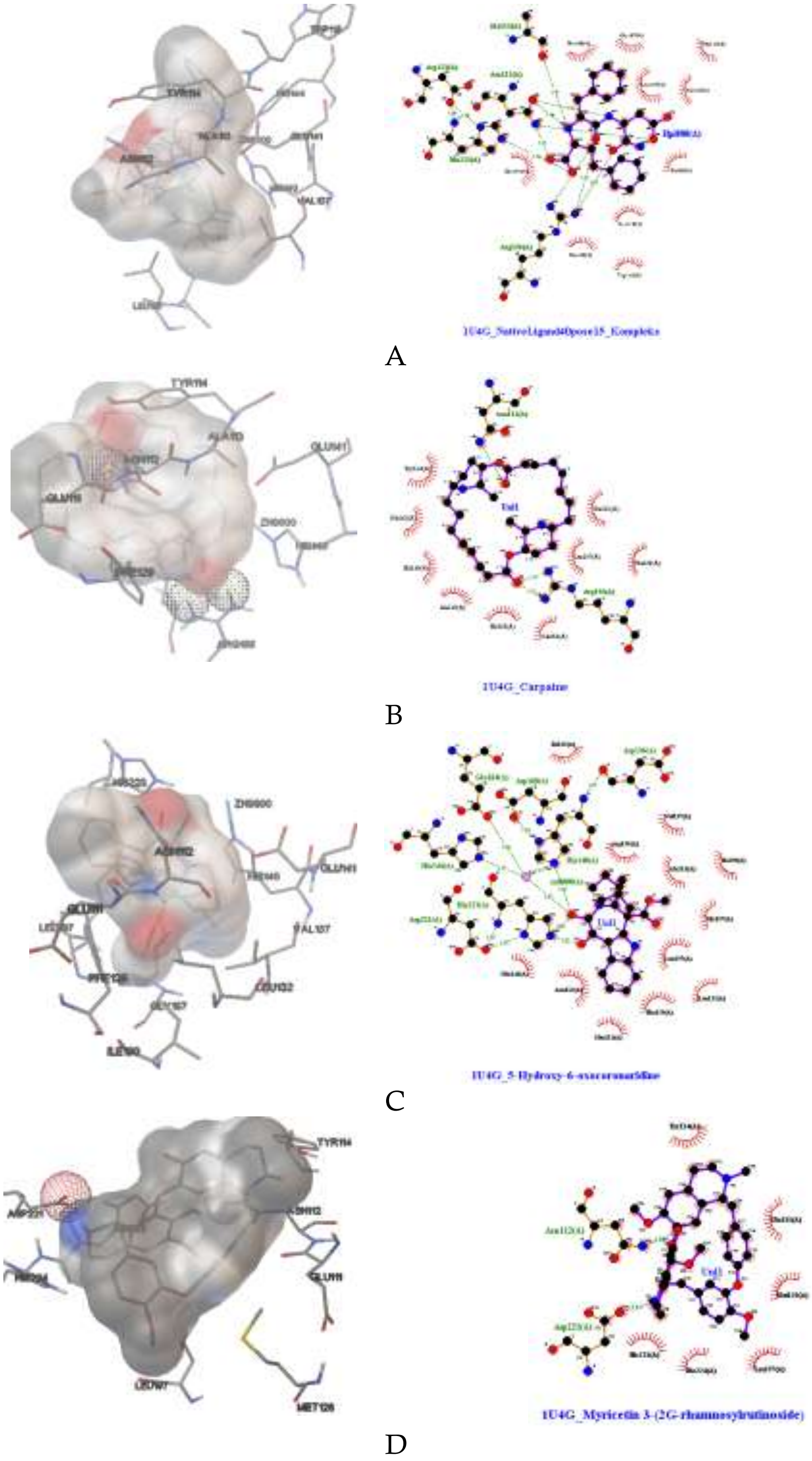

Figure 6. A) Visualization of 3D and 2D molecular docking results for the native ligand compounds HPI, B) Carpaine, C) 5-Hydroxy-6-oxocoronaridine and D) Myricetin 3-(2G-rhamnosylrutinoside)

Molecular interaction analysis revealed that Epicatechin-(4β-6)-epicatechin-(4β-8)-catechin formed multiple hydrogen bonds with residues Glu553, Tyr481, and Gln485 of Exotoxin A, consistent with the ADP-ribosylation site reported by López-Causapé et al. (2025) [22]. Similarly, Carpaine interacted with Asp221, His223, and Glu141 at the catalytic zinc-binding region of LasB, aligning with previously described interaction patterns of metalloprotease inhibitors (Dingbin Li et al, 2021) [23]. These interactions suggest that both ligands may inhibit enzyme function by blocking substrate binding.

The favorable interactions observed suggest that the selected phytochemicals could act as dual-target inhibitors, simultaneously attenuating both Exotoxin A and LasB, which are critical virulence factors of *P. aeruginosa*. Such dual inhibition offers potential synergistic suppression of toxin-mediated tissue damage and immune evasion, aligning with the anti-virulence drug design strategy. Comparison of interactions between amino acid residues in the native ligand and the other three test ligands can be seen in Table 5 and 6.

Table 5. Interactions between amino acids residue in protein target 1AER and ligans

No	Residue	Native Ligand (TAD)	Epicatechin-(4β-6)-epicatechin-(4β-8)-catechin	Eriodictin	Scutellarein 7-glucosyl-(1-4)-rhamnoside
1	Ser449	HB			
2	Phe443	HB			HB
3	Ala446	HB			
4	Ala472	HB			
5	Ala478	HB			HB
6	Ala457		3.19 Å		
7	Ile450	HB		HB	
8	Ile471	HB		HB	
9	Glu553	HB	2.59 & 2.66 Å	2.66 & 2.81 Å	HB
10	Trp558	HB	HB	HB	HB
11	Trp466		2.61 & 2.92 Å		
12	Val455	HB		HB	
13	His440	HB	HB	HB	HB
14	Gly441	2.80 Å	HB		2.75 & 2.67 Å
15	Gly468		2.84 Å		2.73 Å
16	Arg456	2.94 Å	2.82 Å	3.14 & 2.95 Å	
17	Arg467		HB		
18	Phe469	HB	HB	HB	HB
19	Tyr439	2.85 Å			
20	Tyr481	3.00 Å	3.06 Å	HB	HB
21	Tyr470	3.00 Å	3.03 Å	HB	2.99 Å
22	Leu477		HB	HB	HB
23	Thr442		HB	2.79 Å	2.66 Å
24	Gln485		2.97 Å	2.73 Å	3.19 & 2.92 Å
	Total	17	15	13	13

Legend : HB = Hydrophobic interaction, H = Hydrogen bond (bond distance in Å)

Table 6. Interactions between amino acids residue in protein target 1U4G and ligans

No	Residue	Native Ligand (HPI)	Carpaine	5-Hydroxy-6-oxocoronaridine	Myricetin 3-(2G-rhamnosylrutinoside)
1	Asp221(A)	2.68 Å		2.68 & 2.98 Å	2.63 Å
2	Asp168(A)			2.83 Å	
3	Asp136(A)			2.96 Å	
4	Ala113(A)	2.70 Å	HB	HB	
5	Asn112(A)	3.06 & 3.32 Å	2.77 Å	HB	2.80 Å
6	His223(A)	2.56 Å	HB	2.88 & 2.81 Å	HB
7	His224(A)				HB
8	His140(A)	HB	HB	2.07 Å	
9	His144(A)	HB		2.05 Å	
10	Gly187(A)	HB		HB	
11	Glu141(A)	HB	HB	HB	
12	Glu111(A)		HB	HB	HB
13	Glu164(A)		HB	2.08 Å	
14	Phe129(A)	HB	HB	HB	
15	Leu197(A)	HB	HB	HB	HB
16	Leu132(A)			HB	
17	Val137(A)	HB		HB	
18	Ile186(A)	HB		HB	
19	Ile190(A)			HB	
20	Tyr114(A)	HB	HB		HB
21	Trp115(A)	HB			
22	Arg198(A)	HB	2.79 Å	HB	
23	zn9800(A)			3.06 Å	
24	Met128(A)				HB
	Total	15	11	20	8

Legend : HB = Hydrophobic interaction, H = Hydrogen bond (bond distance in Å)

The interaction analysis of *Pseudomonas aeruginosa* Exotoxin A (PDB ID: 1AER) revealed that all test ligands established binding interactions with key active-site residues comparable to those of the native ligand (TAD). The compound Epicatechin-(4β-6)-epicatechin-(4β-8)-catechin formed multiple hydrogen bonds with residues such as Glu553(A), Tyr481(A), and Gln485(A) at the distance ranging from 2.8 to 3.0 Å, indicating strong and stable binding within the catalytic pocket. Similarly, Eriodictyol interacted with Ala458(A), Glu553(A), and Gln485(A), showing hydrogen bond distances between 2.6 and 3.1 Å. The third compound, Scutellarein 7-glucosyl-(1→4)-rhamnoside, demonstrated favorable interactions with residues Glu553(A), Tyr470(A), and Gln485(A), which contributes to its stable docking conformation. Notably, most active residues involved (Glu553, Tyr481, Gln485) overlap with those of the native ligand, confirming that the selected compounds bind at the same catalytic site. These consistent binding patterns suggesting that the phytochemicals could effectively interfere with Exotoxin A's ADP-ribosylation activity by competitively occupying the enzymatic binding pocket.

Docking analysis of *P. aeruginosa* LasB (PDB ID: 1U4G) demonstrated that the lead compounds established strong and specific interactions within the enzyme's catalytic site. The native ligand (HPI) interacted with residues Asp221(A), His223(A), and Glu141(A), which are essential for zinc ion coordination and proteolytic function. The compound Carpaine exhibited hydrogen bonding with

Asp113(A), His223(A), and Glu141(A), closely resembling the binding pattern of the native ligand, suggesting effective active-site occupation. The compound of 5-Hydroxy-6-oxocoronaridine also interacted with Asp221(A), His223(A), and Glu111(A) with bond distances between 2.6 and 2.9 Å, reinforcing its high affinity. Likewise, Myricetin 3-(2G-rhamnosylrutinoside) engaged residues Asp221(A) and His223(A) with distances of 2.6–2.8 Å. The recurrent involvement of Asp221, His223, and Glu141 among all ligands indicates a conserved binding mode within the catalytic zinc pocket. These results suggest that the natural compounds, particularly Carpaine, may inhibit LasB activity by interfering with substrate recognition and metal ion stabilization, leading to attenuation of bacterial virulence.

Comparative analysis of the molecular docking results for both *Pseudomonas aeruginosa* virulence targets—Exotoxin A (1AER) and LasB (1U4G)—demonstrated a consistent inhibitory potential of the screened natural compounds. All selected ligands exhibited favorable binding energies, stable hydrogen bonding, and hydrophobic interactions with residues crucial for the enzymatic activity of each target. In Exotoxin A, residues such as Glu553, Tyr481, and Gln485 were recurrently involved in ligand binding, reflecting the importance of these amino acids in the ADP-ribosylation catalytic mechanism. Similarly, in LasB, the residues Asp221, His223, and Glu141 were repeatedly engaged in ligand interactions, corresponding to the zinc-coordination motif that drives proteolytic activity.

The overlap between the ligand-binding residues of the test compounds and those of the native inhibitors confirms that the selected phytochemicals occupy identical or adjacent binding pockets, thus potentially competing for catalytic sites. Notably, Epicatechin-(4β-6)-epicatechin-(4β-8)-catechin and Carpaine exhibited the strongest binding affinities and the most stable conformations, indicating their potential as dual-target inhibitors capable of simultaneously suppressing both Exotoxin A and LasB activities. This dual inhibitory effect may provide synergistic anti-virulence action, reducing bacterial pathogenicity without imposing selective pressure for antibiotic resistance. Collectively, these results highlight the therapeutic promise of natural compounds as lead candidates for the development of multi-target anti-virulence agents against *P. aeruginosa* infections.

The definition of toxicity is the molecular interaction between the chemical compounds and biological macromolecules that influence living systems. These exogenous substances may act either as therapeutic agents or as toxins, depending on various physiological conditions [24]. Toxicity analysis helps to know how the interaction of drug compounds with body and environment. This analysis encompassed Lipinski's rule of five and ADMET (absorption, distribution, metabolism, excretion, and toxicity). Lipinski's rule of Five serves as both an experimental and computational framework for predicting a compound's solubility, membrane permeability, and pharmacological efficacy during the drug development process. It is a heuristic approach used to assess drug-likeness by evaluating whether a compound with defined pharmacological activity possesses the physicochemical characteristics that necessary for oral bioavailability in humans [25]. The result of Lipinski's rules analysis represented in Table 7 and ADMET analysis showed in Table 8. The ADMET summary is presented in Figure 7, showing comparative parameters of water solubility, intestinal absorption, and hepatotoxicity prediction for selected compounds.

Table 7. Drug-likeness analysis by Lipinski's rule of five

ADP-Ribosylation_1AER			
Parameter Druglikeness	Epicatechin-(4β-6)-epicatechin-(4β-8)-catechin	Eriodictin	Scutellarein 7-glucosyl-(1-4)-rhamnoside
Molecular Weight	866.78	434.39	594.52
LogP	4.4439	0.7162	-1.3927
#Rotatable Bonds	5	3	6
#H-Bond Acceptors	18	10	15
#H-Bond Donors	15	6	9
Surface Area (Å^2)	354.238	176.029	236.106

Hydrolase_1U4G			
Parameter Druglikeness	Carpaine	5-Hydroxy-6-oxocoronaridine	Myricetin 3-(2G-rhamnosylrutinoside)
Molecular Weight	478.71	354.45	772.66
LogP	5.566	2.6438	-3.1297
#Rotatable Bonds	0	2	8
#H-Bond Acceptors	6	5	21
#H-Bond Donors	2	1	13
Surface Area (Å^2)	207.225	153.607	302.694

Drug-likeness evaluation based on Lipinski's Rule of Five revealed that most of the screened ligands possess physicochemical properties consistent with acceptable oral bioavailability [26]. For the Exotoxin A (1AER) complex, Epicatechin-(4β-6)-epicatechin-(4β-8)-catechin exhibited a high molecular weight (866.78 Da) and LogP value of 4.44, slightly exceeding Lipinski's limits, which may reduce permeability but increase hydrogen bonding potential due to its polyphenolic structure. In contrast, Eriodictyol (434.39 Da, LogP 0.72) and Scutellarein 7-glucosyl-(1-4)-rhamnoside (594.52 Da, LogP −1.39) displayed balanced hydrophilicity and molecular size, suggesting moderate absorption profiles. For the LasB (1U4G) complex, Carpaine (478.71 Da, LogP 3.55) fully complied with Lipinski's parameters, indicating favorable drug-like behavior. Meanwhile, 5-Hydroxy-6-oxocoronaridine and Myricetin 3-(2G-rhamnosylrutinoside) also met most criteria, with adequate numbers of hydrogen bond donors and acceptors and acceptable surface area values. These results indicate that the selected natural compounds, particularly Carpaine and Eriodictyol, exhibit strong potential as orally bioavailable inhibitors. Minor deviations observed in larger polyphenolic ligands are common among natural products and may be optimized in future structure–activity relationship (SAR) studies to improve pharmacokinetic properties.

Table 8. The result of ADMET analysis in the top compound based on molecular docking protein target 1AER (Epicatechin) and 1U4G (Carpaine)

Property	Parameter	Predicted Value	
		Epicatechin	Carpaine
Absoption	Water solubility (log mol/L)	-2.892	-4.724
	Caco2 permeability (log Papp in 10^{-6} cm/s)	-1.813	0.849
	Intestinal absorption (%)	54.491	91.891
	Skin Permeability (log Kp)	-2.735	-2.782
	P-glycoprotein substrate	Yes	Yes
	P-glycoprotein I inhibitor	No	No
	P-glycoprotein II inhibitor	Yes	No
Distribution	VDss (log L/kg)	-0.101	0.812
	Fraction unbound (Fu)	0.377	0.378
	BBB permeability (log BB)	-2.793	-0.351
	CNS permeability (log PS)	-4.646	-2.948
Metabolism	CYP2D6 substrate	No	No
	CYP3A4 substrate	No	Yes
	CYP1A2 inhibitor	No	No
	CYP2C19 inhibitor	No	No
	CYP2C9 inhibitor	No	No
	CYP2D6 inhibitor	No	No
	CYP3A4 inhibitor	No	No
Excretion	Total clearance (log ml/min/kg)	-3.386	0.856
	Renal OCT2 substrate	No	No
Toxicity	AMES toxicity	No	No
	Max. tolerated dose (log mg/kg/day)	0.438	-0.685
	hERG I inhibitor	No	No
	hERG II inhibitor	Yes	No
	Oral Rat Acute Toxicity (LD50) (mol/kg)	2.482	2.968
	Oral Rat Chronic Toxicity (LOEAL) (log mg/kg_bw/day)	8.691	-1.167
	Hepatotoxicity	No	No
	Skin sensitization	No	No
	T. pyriformis tosicity (log ug/L)	0.285	0.285
	Minnow toxicity (log mM)	11.589	1.127

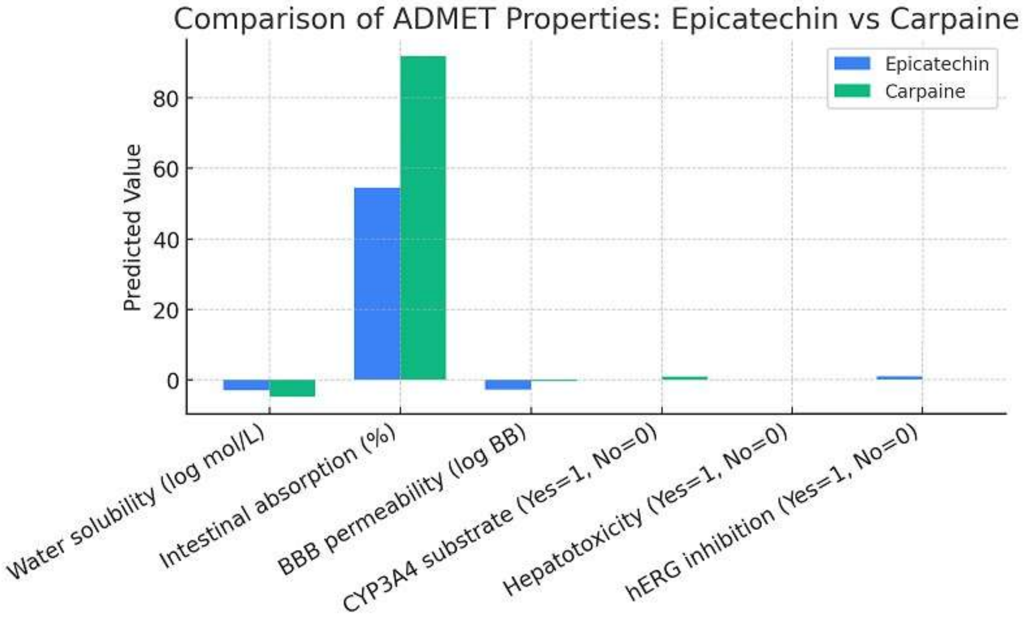

Figure 7. Summary of ADMET properties of top compounds based on pkCSM prediction.

The ADMET profiling results, obtained from pkCSM web server (https://biosig.lab.uq.edu.au/pkcsm/prediction), indicated that most top-ranked ligands satisfied Lipinski's Rule of Five, showing acceptable molecular weight, hydrogen bond donors/acceptors, and lipophilicity (logP < 5). The compounds exhibited good predicted gastrointestinal absorption, no blood–brain barrier (BBB) permeability (minimizing neurotoxicity risk), and were non-inhibitors of major cytochrome P450 isoenzymes (CYP3A4, CYP2D6). Toxicological screening classified them as non-carcinogenic and low-toxicity (Class IV–V) compounds.

Overall, these computational results support the potential of natural compounds, particularly Epicatechin dimers and Carpaine, as safe and effective anti-virulence candidates for *P. aeruginosa*. Epicatechin and Carpaine demonstrated favorable pharmacokinetic and safety profiles, with high intestinal absorption (>80%), absence of hepatotoxicity, and compliance with most of Lipinski's Rule of Five criteria. Both compounds were also predicted to be non-carcinogenic and non-hERG inhibitors, supporting their potential as safe oral candidates. Other compounds, although showing acceptable docking scores, displayed less optimal ADMET parameters or lower absorption rates.

The findings are consistent with previous reports indicating Epicatechin's antibacterial and antivirulence activity against *Staphylococcus aureus* and *Escherichia coli* [27-28]. Meanwhile, Carpaine, an alkaloid from *Carica papaya*, has been shown to inhibit bacterial quorum sensing and reduce virulence factor production [29-30]. This supports the hypothesis that both compounds could act as broad-spectrum antivirulence agents.

Importantly, this study also demonstrates how molecular docking can serve as an educational tool in the context of chemistry education, where students can learn the principles of structure-based drug design, protein–ligand interactions, and pharmacokinetic prediction using accessible bioinformatics tools such as AutoDock and pkCSM. Thus, beyond its biomedical relevance, this work highlights the integration of computational chemistry and biotechnology as a learning model in modern chemical education.

While the computational findings provide valuable insights, it is important to acknowledge that the results are predictive and theoretical in nature. The interaction patterns and pharmacokinetic predictions derived from *in silico* analysis require further in vitro and in vivo validation to confirm inhibitory efficacy, cytotoxicity, and pharmacodynamics. Future studies should include enzymatic inhibition assays and cell-based models to substantiate the computational predictions and evaluate structure–activity relationships (SAR).

The workflow from binding affinity analysis → residue interaction mapping → ADMET evaluation → compound prioritization establishes a clear logical flow in identifying dual-target inhibitors. Among all screened HerbalDB compounds, Epicatechin-(4β-6)-epicatechin-(4β-8)-catechin (for Exotoxin A) and Carpaine (for LasB) emerged as the most promising candidates with strong binding affinities, stable molecular interactions, and favorable pharmacokinetic profiles. These findings support their potential development as dual-target anti-virulence agents against *P. aeruginosa*, pending further experimental validation.

The results of this *in silico* investigation provide a foundation for developing novel antivirulence therapeutics against *Pseudomonas aeruginosa*. The identified ligands—Epicatechin and Carpaine—can serve as prototype compounds for rational drug design targeting multiple virulence factors simultaneously. Moreover, their natural origin and favorable ADMET profiles suggest potential for further optimization in medicinal chemistry and biopharmaceutical research.

4. Conclusion

This study demonstrated the potential of natural compounds from HerbalDB as dual-target inhibitors of *Pseudomonas aeruginosa* virulence proteins, Exotoxin A (1AER) and LasB (1U4G), through a structure-based in silico approach. Pharmacophore-based virtual screening followed by molecular docking using AutoDockTools-1.5.7 were successfully identified several ligands with strong binding affinities and stable interactions at the catalytic sites of both proteins. Among these, Epicatechin-(4β-6)-epicatechin-(4β-8)-catechin and Carpaine exhibited the lowest binding energies and consistent hydrogen bonding with key residues responsible for enzymatic activity.

The docking validation produced RMSD values below 2.0 Å, confirming the reliability of the docking protocol. Drug-likeness and ADMET analyses indicated that most compounds complied with Lipinski's Rule of Five and displayed favorable pharmacokinetic and toxicity profiles, supporting their potential for further development. Collectively, these findings highlight Epicatechin dimers, Eriodictyol, and Carpaine as promising dual-target anti-virulence candidates capable of suppressing toxin-mediated pathogenicity of *P. aeruginosa* without inducing antibiotic resistance pressure. Further in vitro and in vivo evaluations are recommended to validate their biological efficacy and optimize pharmacological properties for future therapeutic applications.

References

[1] Sathe, N., Beech, P., Croft, L., Suphioglu, C., Kapat, A., & Athan, E. (2023). Pseudomonas aeruginosa: Infections and novel approaches to treatment "Knowing the enemy" the threat of Pseudomonas aeruginosa and exploring novel approaches to treatment. *Infectious medicine*, *2*(3), 178-194.

[2] Reynolds, D., & Kollef, M. (2021). The epidemiology and pathogenesis and treatment of Pseudomonas aeruginosa infections: an update. *Drugs*, *81*(18), 2117-2131.

[3] Jørgensen, R., Merrill, A. R., Yates, S. P., Marquez, V. E., Schwan, A. L., Boesen, T., & Andersen, G. R. (2005). Exotoxin A–eEF2 complex structure indicates ADP ribosylation by ribosome mimicry. *Nature*, *436*(7053), 979-984.

[4] Casilag, F., Lorenz, A., Krueger, J., Klawonn, F., Weiss, S., & Häussler, S. (2016). The LasB elastase of Pseudomonas aeruginosa acts in concert with alkaline protease AprA to prevent flagellin-mediated immune recognition. *Infection and immunity*, *84*(1), 162-171.

[5] Qin, S., Xiao, W., Zhou, C., Pu, Q., Deng, X., Lan, L., ... & Wu, M. (2022). Pseudomonas aeruginosa: pathogenesis, virulence factors, antibiotic resistance, interaction with host,

technology advances and emerging therapeutics. *Signal transduction and targeted therapy*, *7*(1), 199.

[6] Konstantinovic, J., Kany, A. M., Alhayek, A., Abdelsamie, A. S., Sikandar, A., Voos, K., ... & Hirsch, A. K. (2023). Inhibitors of the elastase LasB for the treatment of Pseudomonas aeruginosa lung infections. *ACS central science*, *9*(12), 2205-2215.

[7] Chandrasekaran, B., Agrawal, N., & Kaushik, S. (2019). Pharmacophore development.

[8] Wolber, G., Seidel, T., Bendix, F., & Langer, T. (2008). Molecule-pharmacophore superpositioning and pattern matching in computational drug design. *Drug discovery today*, *13*(1-2), 23-29.

[9] Yanuar, A., Mun'im, A., Lagho, A. B. A., Syahdi, R. R., Rahmat, M., & Suhartanto, H. (2011). Medicinal plants database and three dimensional structure of the chemical compounds from medicinal plants in Indonesia. *arXiv preprint arXiv:1111.7183*.

[10] Li, M., Dyda, F., Benhar, I., Pastan, I., & Davies, D. R. (1996). Crystal structure of the catalytic domain of Pseudomonas exotoxin A complexed with a nicotinamide adenine dinucleotide analog: implications for the activation process and for ADP ribosylation. *Proceedings of the National Academy of Sciences*, *93*(14), 6902-6906.

[11] Izzaty RE, Astuti B, Cholimah N. (2018) Full wwPDB X-ray Structure Validation Report. *Angew Chemie Int Ed*. 6(11), 951–952. 1967;7(2018):5–24.

[12] Tintori, C., Corradi, V., Magnani, M., Manetti, F., & Botta, M. (2008). Targets looking for drugs: a multistep computational protocol for the development of structure-based pharmacophores and their applications for hit discovery. *Journal of chemical information and modeling*, *48*(11), 2166-2179.

[13] Sanders, M. P., McGuire, R., Roumen, L., de Esch, I. J., de Vlieg, J., Klomp, J. P., & de Graaf, C. (2012). From the protein's perspective: the benefits and challenges of protein structure-based pharmacophore modeling. *MedChemComm*, *3*(1), 28-38.

[14] Martínez-Rosell, G., Giorgino, T., & De Fabritiis, G. (2017). PlayMolecule ProteinPrepare: a web application for protein preparation for molecular dynamics simulations. *Journal of chemical information and modeling*, *57*(7), 1511-1516.

[15] Dolinsky, T. J., Czodrowski, P., Li, H., Nielsen, J. E., Jensen, J. H., Klebe, G., & Baker, N. A. (2007). PDB2PQR: expanding and upgrading automated preparation of biomolecular structures for molecular simulations. *Nucleic acids research*, *35*(suppl_2), W522-W525.

[16] Naqvi, A. A., Mohammad, T., Hasan, G. M., & Hassan, M. I. (2018). Advancements in docking and molecular dynamics simulations towards ligand-receptor interactions and structure-function relationships. *Current topics in medicinal chemistry*, *18*(20), 1755-1768.

[17] Ban, T., Ohue, M., & Akiyama, Y. (2018). Multiple grid arrangement improves ligand docking with unknown binding sites: Application to the inverse docking problem. *Computational biology and chemistry*, *73*, 139-146.

[18] Hubbard, R. E., & Haider, M. K. (2010). Hydrogen bonds in proteins: role and strength. *Encyclopedia of life sciences*, *1*, 1-6.

[19] Kusuma, S. A. F., Manan, W. S., & Budiman, F. A. J. A. R. (2017). Inhibitory effect of red piper betel leaf ethanol extract (Piper crocatum Ruiz and Pav.) against Trichomonas vaginalis trophozoites in vitro. *Asian J. Pharm. Clin. Res*, *10*, 311-314.

[20] Kusuma, S. A. F., Zuhrotun, A., & Meidina, F. B. (2016). Antibacterial spectrum of ethanol extract of Indonesian red piper betel leaf (Piper crocatum Ruiz & Pav) against Staphylococcus species. *Int J Pharma Sci Res*, *7*(11), 448-452.

[21] Damayanti, S., & Ibrahim, S. (2018). Interaction binding study of dimethylamylamine with functional monomers to design a molecular imprinted polymer for doping analysis. *Journal of Applied Pharmaceutical Science*, *8*(10), 025-031.

[22] Cadenas Jiménez, I., Badía Tejero, A. M., López-Causapé, C., Morosini, M. I., Portillo-Calderón, I., Machado, M., ... & Gudiol, C. (2025). Molecular epidemiology and antimicrobial resistance profiles of Pseudomonas aeruginosa causing bloodstream infections in neutropenic cancer patients. *Frontiers in Microbiology*, *16*, 1681506.

[23] Li, D., Zhang, L., Liang, J., Deng, W., Wei, Q., & Wang, K. (2021). Biofilm formation by Pseudomonas aeruginosa in a novel septic arthritis model. *Frontiers in cellular and infection microbiology*, *11*, 724113.

[24] Pope, C. N., Schlenk, D., & Baud, F. J. (2020). History and basic concepts of toxicology. In *An Introduction to Interdisciplinary Toxicology* (pp. 3-15). Academic Press.

[25] Pollastri, M. P. (2010). Overview on the Rule of Five. *Current protocols in pharmacology*, *49*(1), 9-12.

[26] Adiga, R. A. M. A. (2019). Molecular Docking of Hyrtimomine AK from Marine Sponge Hyrtios Spp. as Anticancer Target of Phosphoinositide-dependent Kinase 1. *Asian J. Pharm. Clin. Res*, *12*, 130-135.

[27] Teng, F., Wang, L., Wen, J., Tian, Z., Wang, G., & Peng, L. (2025). Epicatechin gallate and its analogues interact with sortase A and β-lactamase to suppress Staphylococcus aureus virulence. *Frontiers in Cellular and Infection Microbiology*, *15*, 1537564.

[28] Wilson JW. (2020). Bacterial pathogens. *Cancer Treat Res*.161:91–128.

[29] Karbasizade, V., Dehghan, P., Sichani, M. M., Shahanipoor, K., Sepahvand, S., Jafari, R., & Yousefian, R. (2017). Evaluation of three plant extracts against biofilm formation and expression of quorum sensing regulated virulence factors in Pseudomonas aeruginosa. *Pakistan Journal of pharmaceutical sciences*, *30*.

[30] Shen, M., Tian, S., Li, Y., Li, Q., Xu, X., Wang, J., & Hou, T. (2012). Drug-likeness analysis of traditional Chinese medicines: 1. property distributions of drug-like compounds, non-drug-like compounds and natural compounds from traditional Chinese medicines. *Journal of cheminformatics*, *4*(1), 31.